NJC

Accepted Manuscript

This article can be cited before page numbers have been issued, to do this please use: Y. Wang, Z. Yang, F. Zhan, Z. LYu, C. Han, X. Wang, W. Chen, M. Ding, R. Wang and Y. Jiang, *New J. Chem.*, 2018, DOI: 10.1039/C8NJ02505C.

ROYAL SOCIETY OF CHEMISTRY

rsc.li/njc

View Article Online
DOI: 10.1039/C8NJ02505C

Indolizine Quaternary Ammonium Salt Inhibitors: A reinvestigation of an Old Fashioned Strong Acid Corrosion Inhibitor Phenacyl Quinolinium Bromide and Its Indolizine Derivative

Yefei Wang[*,1], *Zhen Yang*[1], *Fengtao Zhan*[2], *Zhifeng LYu*[2], *Chengyou Han*[2], *Xiaonuo Wang*[2], *Wuhua Chen*[1], *Mingchen Ding*[1], *Renzhuo Wang*[1], *Yingnan Jiang*[3]

[1]College of Petroleum Engineering, China University of Petroleum (East China), 66 West Changjiang Rd, Qingdao, Shandong Province, 266580, P. R. China

[2]College of Science, China University of Petroleum (East China), 66 West Changjiang Rd, Qingdao, Shandong Province, 266580, P. R. China

[3]College of Computer Engineering, Cinema and Mechatronics, Politecnico di Torino, 24 Corso duca degli abruzzi, Torino, 10129, Italy

View Article Online
DOI: 10.1039/C8NJ02505C

ABSTRACT: Phenacyl Quinolinium Bromide (PaQBr), an old-fashioned corrosion inhibitor in strong acid medium was reinvestigated and a new indolizine derivative (DiPaQBr) was synthesized from PaQBr. The DiPaQBr is classified as an indolizine quaternary ammonium salt. Based on High Resolution Mass Spectrometry (HRMS) and NMR, the formula and chemical structure of DiPaQBr was accurately confirmed and characterized. The formation mechanism of DiPaQBr from the condensation of two molecules of PaQBr through 1,3-dipolar cycloaddition was proposed. The corrosion inhibition of PaQBr and DiPaQBr on N80 steel in 15% HCl was investigated by weight loss measurement, potentiodynamic polarization and electrochemical impedance spectroscopy (EIS). Polarization results indicate that the examined two compounds are of mixed-type inhibitor. The adsorption of the studied inhibitors obeyed the Langmuir adsorption isotherm. The obtained results from gravimetric research as well as electrochemical study indicated that compared with the inhibitive PaQBr, its indolizine derivative DiPaQBr could exhibit a better corrosion prevention performance at a much lower concentration. The achieved results indicate that the derivative (indolizine quaternary ammonium salt) of heterocyclic quaternary ammonium salts would inhibit the steel more effectively in acid medium.

KEYWORDS: Acid inhibition; N80 Steel; Phenacyl Quinolinium Bromide; Indolizine derivative;

1. Introduction

New corrosion inhibitors for acidizing (≥15 wt.% hydrochloric acid as the working fluid at 90℃ or higher temperature) in petroleum industry are in great demand as the EOR technique develops.[1-4] Among the numerous corrosion inhibitors, nitrogen-containing heterocyclic quaternary ammonium salts have been generally used to prevent N80 steel from getting severely

View Article Online
DOI: 10.1039/C8NJ02505C

corroded in acidizing engineering.[2-6] These quaternary ammonium salts are usually synthesized by nitrogen-containing heterocyclic bases (pyridine, quinoline or their derivatives) and series of halogenated compounds through quaterisation reaction.[7-9]

For decades, the BQC (Benzyl Quinolinium Chloride) served as a commonly used inhibitor for acidizing. In our previous work,[1,10] we have reported that the BQD (Benzyl Quinolinium Chloride Derivative), a dimer derivative of BQC, would be formed by the condensation of two BQC molecules (Fig. 1). Compared with BQC, the protection performance of BQD in 15 wt.% HCl gets dramatically promoted. However, the formation mechanism of BQD was ambiguous since the chemical structure of BQD was not fully studied and assigned accurately in previous work.

As illustrated in Fig. 1, in this paper, the dimer derivative (like BQD) is redefined as the indolizine derivative (indolizine quaternary ammonium salt) according to literatures.[11-13] Heterocyclic quaternary ammonium salts which possess active methylene group (like BQC) would easily get converted to their corresponding indolizine derivatives (like BQD) via 1,3-dipolar cycloaddition.[14-19]

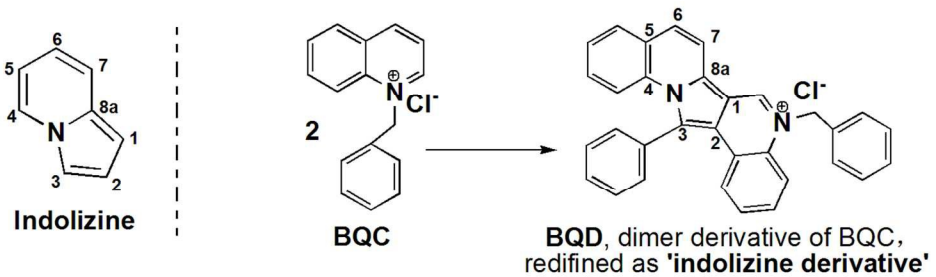

Fig. 1 Structure of Indolizine and the formation of BQD from BQC.

The great difference of corrosion inhibition between BQC and BQD[1] implies that similar dimer derivative of BQD may also exhibit a better inhibition performance than the precursor heterocyclic quaternary ammonium salts inhibitors. In order to further confirm the hypotheses,

View Article Online
DOI: 10.1039/C8NJ02505C

heterocyclic quaternary ammonium salt with active methylene group is the appropriate target compound to investigate. R.I. Yurchenko et al. had once studied the inhibitive behavior of Phenacyl Quinolinium Bromide (PaQBr, Fig. 2) for 08 KP steel in 3 M H_2SO_4, indicating its effective inhibition in acid medium.[20-22] Owning to the electronegative effect of quaternary N^+ atom as well as the carbonyl group in PaQBr, the active methylene group in PaQBr could be transformed to its N-Ylide structure easily.[23-27] The active N-Ylide intermediate would thereby react with another molecule of PaQBr under certain condition to form a corresponding indolizine quaternary ammonium salt (the dimer derivative of PaQBr, DiPaQBr, see Fig. 2), whose structure is very similar with BQD.[1,14,28-36]

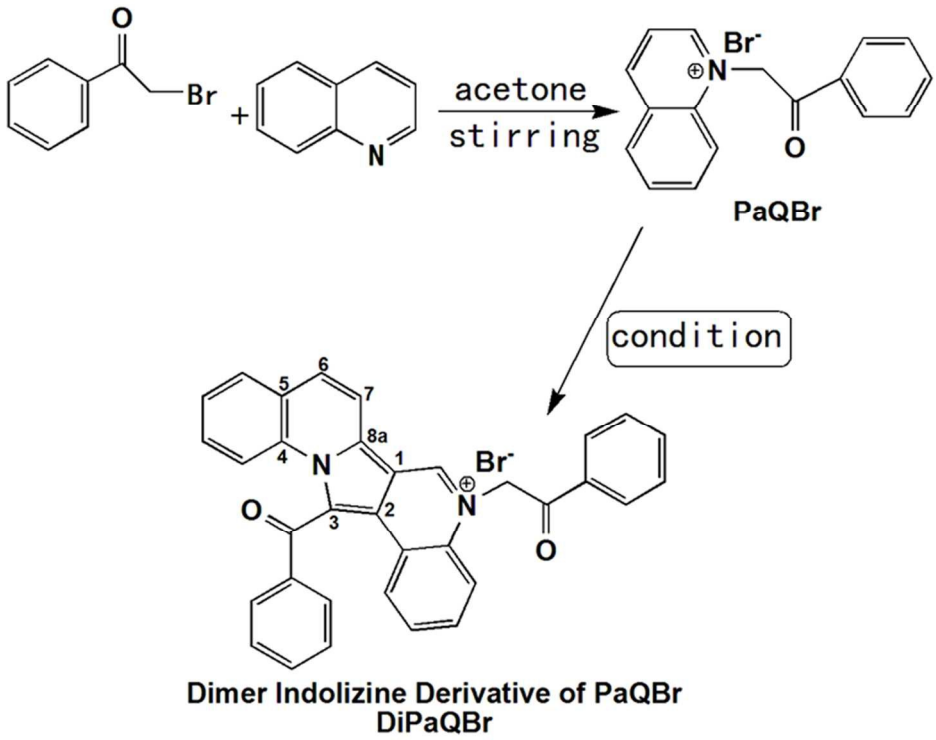

Fig. 2 Synthesis of Phenacyl Quinolinium Bromide (PaQBr) and its dimer derivative, DiPaQBr.

In this study, PaQBr was synthesized and its indolizine quaternary ammonium salt DiPaQBr was obtained with the assistance of triethylamine. The structure of DiPaQBr was confirmed by High Resolution Mass Spectrometry (HRMS) and NMR. The formation mechanism of DiPaQBr

View Article Online
DOI: 10.1039/C8NJ02505C

from PaQBr was characterized as 1,3-dipolar cycloaddition.[11,33] The inhibition ability of PaQBr and DiPaQBr in 15 wt.% HCl for N80 steel is investigated via weight loss measurement, Tafel polarization measurements and electrochemical impedance spectroscopy (EIS). The possible inhibitive mechanism of the two compounds is discussed.

2. Experimental section

2.1 Preparation of PaQBr and DiPaQBr.

0.1 mol quinoline was mixed with 0.1 mol 2-bromoacetophenone in a 250 mL three-necked flask. Then approximately 20 mL of acetone was added to the flask as solvent. The reaction mixture was stirred at room temperature for 6 hours, and then a large amount of light brown solution with yellow precipitate was obtained.[37-39] The yellow product was washed with acetone and recrystallized with alcohol. Pure phenacyl quinolinium bromide (PaQBr) was obtained as light yellow powder. The chemical structure of PaQBr was confirmed by NMR (Agilent NMR-400 MHz).

Phenacyl Quinolinium Bromide (PaQBr): Yield 85.9%, m.p. 166 °C (decomposed), solubility: 15.8 g/100mL in water. ^{1}H NMR (400 MHz, DMSO-d_6):δ9.67 (d, J = 5.9 Hz, 1H), 9.51 (d, J = 8.3 Hz, 1H), 8.59 (d, J = 6.8 Hz, 1H), 8.49 (d, J = 9.0 Hz, 1H), 8.36 (dd, J = 8.4, 5.8 Hz, 1H), 8.22 (dd, J = 18.9, 7.2 Hz, 3H), 8.07 (t, J = 7.6 Hz, 1H), 7.84 (t, J = 7.4 Hz, 1H), 7.71 (t, J = 7.7 Hz, 2H), 7.16 (s, 2H). ^{13}C NMR (101 MHz, DMSO-d_6):δ191.29, 151.42, 149.03, 139.11, 136.38, 135.29, 134.09, 131.08, 130.43, 129.86, 129.54, 129.17, 122.65, 119.67, 63.80.

5 g PaQBr and 0.5g triethylamine was dissolved with acetonitrile in a three-necked flask. The mixture was heated and kept at 70℃ for 1 hour, and then the solution became dark reddish. Afterwards, the acetonitrile was evaporated and a solid pigment-like mixture was obtained. A

View Article Online
DOI: 10.1039/C8NJ02505C

silica gel column chromatography was used to isolate the pigment-like mixture and the solvent was iso-propanol–chloroform (1:9, v/v).

Thin layer chromatography (TLC) with the same solvent as in column chromatography was used to monitor the eluate of column chromatography. Compared with BQD,[1] the DiPaQBr was also viewed as light fluorescent yellow point at ultraviolet light and the R_f value of DiPaQBr was approximately 0.65. Finally, the yellow eluates containing DiPaQBr were evaporated at reducing pressure, and the DiPaQBr was obtained as dark orange solid. The chemical structure of DiPaQBr was confirmed by NMR (Agilent NMR-400 MHz).

Dimer Derivative of Phenacyl Quinolinium Bromide (DiPaQBr): Yield 23.2% (approximately), m.p. 208 °C (decomposed), slightly soluble in water. ^{1}H NMR (400 MHz, $CDCl_3$):δ11.93 (s, 1H), 9.00 (d, J = 9.0 Hz, 1H), 8.28 (d, J = 7.7 Hz, 2H), 8.19 (d, J = 8.2 Hz, 1H), 8.08 (d, J = 8.9 Hz, 1H), 7.99 (dd, J = 10.9, 7.1 Hz, 2H), 7.76 (d, J = 7.8 Hz, 2H), 7.72-7.50 (m, 8H), 7.41 (t, J = 7.3 Hz, 3H), 7.16 (s, 2H). ^{13}C NMR (101MHz, $CDCl_3$):δ191.17, 190.95, 150.04, 136.91, 135.82, 135.24, 134.85, 134.56, 133.84, 132.33, 130.93, 130.57, 130.40, 130.09, 129.69, 129.67, 129.26, 128.85, 128.48, 127.46, 126.99, 126.55, 123.20, 120.80, 120.77, 119.29, 118.56, 117.10, 109.99, 61.88.

2.2 Preparation of the acid solution and specimens.

15 wt.% hydrochloric acid solution was chosen as corrosive medium for both the weight loss measurements and the electrochemical experiments . The acid solution was prepared by dilution of 36-38 wt.% commercially available analytical grade hydrochloric acid with double distilled water. The composition of N80 specimens was as follows: (in wt.%) Cr, 0.20; Mn, 0.92; S, 0.008; P, 0.01; Si, 0.19; C, 0.31; and Fe, balance. The dimension of the N80 steel specimens for the weight loss analysis was 50 mm×10 mm×3 mm. The same specimens with 10 mm^2 exposed

View Article Online
DOI: 10.1039/C8NJ02505C

surface areas were used as working electrodes for electrochemical measurements. The exposed area of the specimens was mechanically abraded with increasing grades of emery papers (600, 800, 1200 and 2000 grit), followed by cleaning in turn with double distilled water, acetone and ethanol, and finally dried at room temperature before the inhibition experiments.

2.3 Weight loss measurement.

After the weighting, the specimens were suspended in 15 wt.% HCl solutions with and without different concentrations of PaQBr or DiPaQBr for 4 h at 90 °C, in which the ratio of volume (mL) of acid solutions to surface area (cm^2) of the specimen was 20:1. The experiments were carried out in triplicates in each test and only the average value of corrosion rate was used in calculations. The corrosion rate (ν_{corr}) in g m^{-2} $h^{-1}$of each specimen was calculated from the following equation:

$$\nu_{corr} = \frac{W_1 - W_2}{S \times t} \qquad (1)$$

where, ν_{corr} = corrosion rate (g m^{-2} h^{-1}), W_1 (g) and W_2 (g) =weights of a specimen before and after the 4h experiment respectively, S = surface area of the specimen (m^2), t =immersion time (h).

2.4 Electrochemical measurements.

Electrochemical analysis was carried out on Gamry Reference 600 electrochemical work station in 15 wt.% HCl solution at 25°C under non-stirred conditions. Three-electrode corrosion cell including N80 steel (1 cm^2 exposed surface area) as a working electrode (WE), SCE (saturated calomel electrode coupled to a fine Luggin capillary) as a reference electrode (RE), and a platinum counter electrode (CE) was employed to conduct the electrochemical test. The Luggin capillary was kept close to the working electrode to decrease IR drop. All the

View Article Online
DOI: 10.1039/C8NJ02505C

electrochemical experiments were performed in the absence and presence of PaQBr or DiPaQBr at the concentrations as same as those for weight loss measurement.

The three-electrode cell was immersed in each test solution for 20 min in order to ensure a stable open circuit potential (OCP), and after this, both the potentiodynamic polarization and the EIS measurements were performed at OCP. All the electrochemical data are presented without iR correction. The anodic and cathodic polarization curves were obtained in the potential range from -200 mV to +200 mV versus OCP at an automatically scanning rate of 0.5 mV s^{-1}. The corrosion current density (I_{corr}) and corrosion potential (E_{corr}) were measured by Tafel liner extrapolation procedure. The EIS measurements were taken for the frequency spectrum from 100 kHz to 10 mHz, using an AC amplitude signal of 5 mV peak-to-peak. The EIS experimental data was analyzed using ZSimpWin software.

3. Results and discussion

3.1 Formation of DiPaQBr from PaQBr

3.1.1 Structure characterization of PaQBr

The synthesis of PaQBr is carried out according to the reaction in Fig. 2.

From the ^{13}C-NMR spectrum of PaQBr (see Fig. S1 in Electronic Supplementary Information, ESI) in DMSO-d_6, there is one signal of aliphatic carbon at 63.80 ppm, corresponding to the active -CH_2- carbon next to the quaternary N^+ atom.[40] Thirteen signals of aromatic carbons ranging from 119.67-151.42 ppm are assigned to the fifteen sp^2 aromatic carbon atoms in PaQBr, two of which at 129.17 and 129.54 ppm are overlapped signals represent two carbon atoms respectively. The distinctive signal at 191.29 ppm belongs to the carbonyl group in PaQBr, which emerges at low field area, showing a strong electronegative effect of its chemical environment.

View Article Online
DOI: 10.1039/C8NJ02505C

3.1.2 Structure characterization of DiPaQBr

The platform of HRMS (High Resolution Mass Spectrometry, electrospray ionization, positive ion mode) was used to determine the mass of the molecular ion of DiPaQBr.

The HRMS spectrum of DiPaQBr is shown in Fig. S2, ESI. The HRMS result (positive ion mode) of DiPaQBr shows that its molecular ion peak is m/z 491.1755 and the elemental composition is $[C_{34}H_{23}N_2O_2]^+$.

The ^{1}H-NMR spectrum of DiPaQBr (Fig. S3, ESI) in $CDCl_3$ shows a signal at 7.16(2H), corresponding to the protons on -CH_2- group next to the quaternary N^+ atom. Signals at 7.41 (3H), 7.57-7.70 (8H), 7.75 (2H), 7.99 (2H), 8.08 (1H), 8.19 (1H), 8.28 (2H), 9.00 (1H) are assigned to the aromatic protons in DiPaQBr. The signal at 11.93(1H) is assigned to the aromatic proton directly attached to the N^+ atom. From the ^{13}C-NMR spectrum of DiPaQBr (Fig. S4, ESI), there is one signal of aliphatic carbon at 61.88 ppm which represents the -CH_2- carbon. Twenty-nine signals from 109.99-191.17 ppm belong to thirty-one sp^2 aromatic carbon atoms and two carbonyl carbons in DiPaQBr, four of which at 128.85, 129.26, 129.67 and 129.69 ppm are overlapped signals represent two carbon atoms respectively. It is apparent that the DiPaQBr molecule contains thirty-four carbon atoms, which is in good agreement with the result of HRMS.

The type of carbon atom (primary, secondary and tertiary carbon) could be accurately identified from the DEPT experiment. DEPT spectrum is a kind of special ^{13}C-NMR spectrum. Quaternary carbon signals could not be found in all DEPT spectrums. The DEPT 90° spectrum displays tertiary carbon only, while primary/tertiary carbon gives signal upwards and secondary carbon gives signal downwards in DEPT 135° spectrum. The results of DEPT experiment are shown in Fig. S5 (a) and Fig. S5 (b), ESI.

View Article Online
DOI: 10.1039/C8NJ02505C

DEPT 135° spectrum indicates seventeen different signals of aromatic tertiary carbons at 150.04, 135.24, 134.85, 130.93, 130.57, 130.40, 130.09, 129.69, 129.67, 129.26, 128.85, 128.48, 127.46, 126.55, 119.29, 118.56, 117.10 ppm and one signal of one aliphatic secondary carbon at 61.88 ppm, four of which at 128.85, 129.26, 129.67 and 129.69 ppm are the overlapped signals represent two carbon atoms respectively. According to DEPT 90° and DEPT 135° spectrum, conclusion can be made that there is no primary carbon in DiPaQBr. It could be easily recognized that signals of the twelve quaternary carbons (191.17, 190.95, 136.91, 135.82, 134.56, 133.84, 132.33, 126.99, 123.20, 120.80, 120.77 and 109.99 ppm) in ^{13}C-NMR spectrum of DiPaQBr could not be observed in both DEPT 90° and DEPT 135° spectrum. The chemical shifts of these twelve quaternary carbons are marked in Fig. S5 (b), ESI.

As a result, from all the data above it is clear that the DiPaQBr molecule contains thirty-four carbon atoms, which comprise two carbonyl carbons, ten aromatic quaternary carbons, a single carbon atom belongs to aliphatic -CH_2- structure and twenty-one aromatic tertiary carbons.

The chemical structure of DiPaQBr (CAS Registry Number was not found) can be concluded from the spectrum results and related references.[22-32] The formation mechanism of DiPaQBr is shown in Fig. 3.

View Article Online
DOI: 10.1039/C8NJ02505C

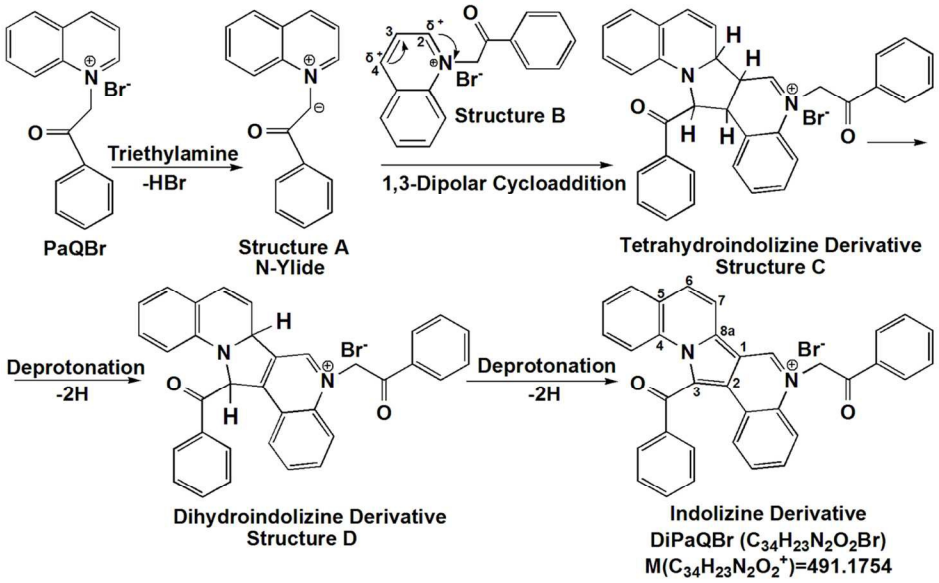

Fig. 3 The formation mechanism of DiPaQBr from PaQBr.

3.1.3 The formation mechanism of DiPaQBr

Fig. 3 illustrates the formation mechanism of DiPaQBr. Owning to the strong electronegativity of the carbonyl group and the quaternary N^+ atom in PaQBr, the PaQBr is easily to get transformed to its corresponding N-Ylide (structure A) in alkaline condition.[23-27] Meanwhile, strong electron-withdrawing conjugated effect engender the partial positive charges at 2-position and 4-position of PaQBr (structure B).[14,18] The induced dipole between 3-position and 4-position of the structure B could be attacked by structure A via 1,3-dipolar cycloaddition reaction and form a cyclized intermediate tetrahydroindolizine derivative[12,28-32] (structure C). The structure C could easily be deprotonated gradually and the dihydroindolizine derivative (structure D) is formed first.[41-43] Then structure D will undertake a further deprotonation process[44] until the final product indolizine derivative (DiPaQBr, $C_{34}H_{23}N_2O_2Br$) is formed. Considering that the DiPaQBr and BQD[1] both comprises the indolizine structure (Fig. 1) and a quaternary N^+ atom, similar compounds could be classified as the indolizine quaternary ammonium salts.

3.2 Weight loss measurement

View Article Online
DOI: 10.1039/C8NJ02505C

The mean value of corrosion rate (ν_{corr}), inhibition efficiency (η) as well as the surface coverage (θ) are obtained from weight loss measurements of N80 steel in 15 wt.% HCl with and without various concentrations of PaQBr or DiPaQBr. Table 1 shows the results of weight loss measurements. The inhibition efficiency (η) and surface coverage (θ) of each inhibitor was determined as the following equation[45]:

$$\theta = \eta = \frac{\nu_0 - \nu_{\mathrm{corr}}}{\nu_0} \times 100 \qquad (2)$$

where, ν_0 (g m^{-2} h^{-1}) and ν_{corr} (g m^{-2} h^{-1}) stands for the corrosion rates of N80 steel without and with inhibitor respectively.

With the increasing concentrations for both of the inhibitors, the result in Table 1 shows that the inhibitors would exhibit a better anticorrosive activity at a higher concentration. For all the concentrations of PaQBr, the corrosion rate (ν_{corr}) of N80 steel decreases to lower values compared with BQC[1] under the same experimental condition, revealing that PaQBr presents a much better corrosion protection than BQC in strong acid solution. It could be inferred that the conjugated molecular skeleton and the synergistic effect of the Br^- ion are the two main reasons to explain the considerable protection efficiency of PaQBr.

The inhibition property of inhibitor usually could be enhanced by heteroatoms (N, O or P et al.) or conjugated organic groups.[46] Compared with BQC, the carbonyl double bond structure in PaQBr provides an extra oxygen item and more π-electrons as adsorbing sites in the inhibition action. Meanwhile, it is widely accepted that the synergistic effect of the halide anions with the inhibitive quaternary cations increases in the order $Cl^- < Br^- < I^-$,[47] indicating that the presence of Br^- (from PaQBr) in the corrosive medium may further improve the inhibition efficiency of the quaternary ammonium inhibitors.

View Article Online
DOI: 10.1039/C8NJ02505C

In Table 1, it is worth observing that compared with PaQBr, the corrosion rate does not decrease apparently as the concentration of DiPaQBr increases. The reason for this could be that the hydrophobic double carbonyl groups and fused-ring aromatic structure in DiPaQBr make it harder to get dissolved.[21-22] The corrosion rate of N80 steel in Table 1 decreased to 634.96 g m^{-2} h^{-1} (inhibition efficiency is 47.5%) when the concentration of DiPaQBr was 0.356 mM. However, when the concentration of PaQBr was 3.559 mM, the corrosion rate of the steel merely reached 798.94 g m^{-2} h^{-1} (inhibition efficiency is 34%). As an indolizine derivative of PaQBr, the presence of DiPaQBr could reduce the corrosion rate more apparently at a lower concentration compared with PaQBr, indicating that the DiPaQBr is a relatively more effective corrosion inhibitor than the precursor quaternary ammonium salt inhibitor (PaQBr).

Table 1 Weight loss results for N80 steel in 15 wt.% HCl at 90 °C in the absence and presence of inhibitor for 4h

substance	Conc. (mM)	v (g m^{-2} h^{-1})	θ	η (%)	Error (%)
15% HCl	0	1210.14			0.79
PaQBr	3.559	798.94	0.3398	34.0	1.13
	8.873	450.42	0.6278	62.8	0.97
	17.771	213.11	0.8239	82.4	1.27
	26.619	139.53	0.8847	88.5	1.15
	35.591	64.74	0.9465	94.7	1.98
DiPaQBr	0.036	966.91	0.2011	20.1	1.88
	0.089	829.68	0.3144	31.4	2.07
	0.177	709.75	0.4135	41.4	1.62
	0.267	667.15	0.4487	44.9	0.97
	0.356	634.96	0.4753	47.5	1.85

3.3 Open circuit potential measurement

The variation of OCPof the N80 working electrode with time in 15 wt.% HCl in the absence and presence of PaQBr or DiPaQBr is graphically presented in Fig. 4. Apparently, the value of

View Article Online
DOI: 10.1039/C8NJ02505C

OCP in uninhibited acid solution is more negative than that in inhibited medium and gradually remained unchanged.

With the addition of the two inhibitors, the steady-state potential moves to a relatively positive direction, suggesting that a high resistance of the charge transfer is taking place on the steel surface. Additionally, it is clear from Fig. 4 that the positive shift of OCP is concentration dependent, since the steady OCP became less negative with increasing concentrations of PaQBr or DiPaQBr.

The OCP-time relationships show that it took about 15 min for the OCPs to reach an unchanged steady state. As a result, during the following electrochemical measurements, the working electrode was immerged in the test solution for 20 min to obtain the steady OCP.

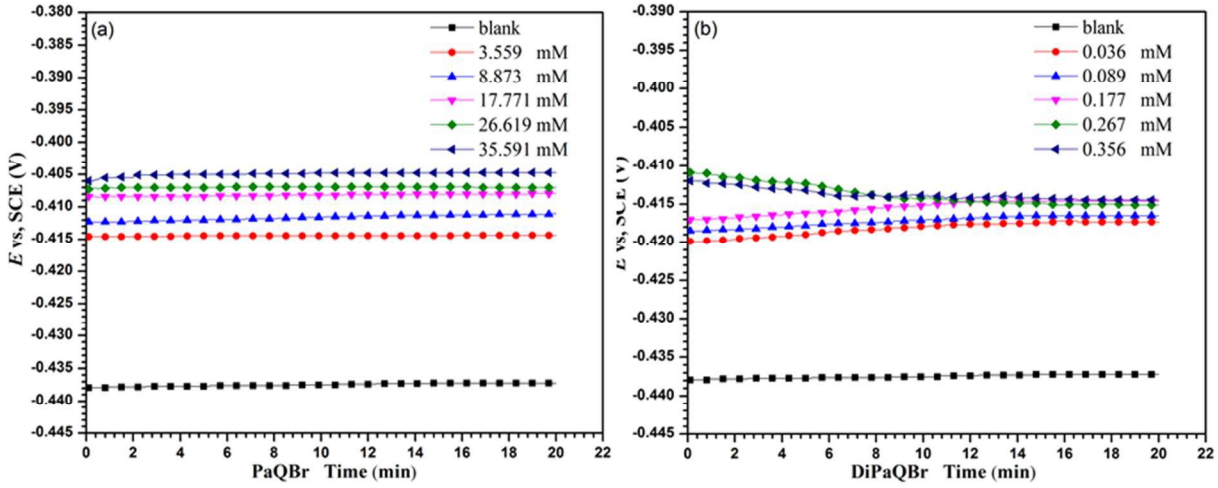

Fig. 4 OCP-time curves for N80 steel in 15 wt.% HCl without and with different concentrations of (a) PaQBr, (b) DiPaQBr at 25 °C.

3.4 Potentiodynamic polarization measurement

The inhibition efficiency from the polarization curves for both inhibitors was determined as the following equation[48]:

$$\eta = \frac{I_{corr} - I'_{corr}}{I_{corr}} \times 100 \qquad (3)$$

View Article Online
DOI: 10.1039/C8NJ02505C

where, I_{corr} and I'_{corr} stands for the mean corrosion current densities in the absence and presence of PaQBr (or DiPaQBr), respectively.

The polarization curves of N80 steel in 15 wt.% HCl solution at 25°C are shown in Fig. 5. The corrosion current density (I_{corr}), the corrosion potential (E_{corr}), the anodic Tafel slopes (b_a), the cathodic Tafel slopes (b_c) and the inhibition efficiency (η) calculated from the curves are given in Table 2.

As shown in Fig. 5(a) and 5(b), the log I values of both cathodic and anodic parts moved to more negative area when the inhibitor exists. It clears from Fig. 5 that both the cathodic and anodic reactions were suppressed by PaQBr and DiPaQBr, which suggests that the two inhibitors reduces the dissolution process of anodic region and retards the cathodic hydrogen evolution reaction as well.[49]

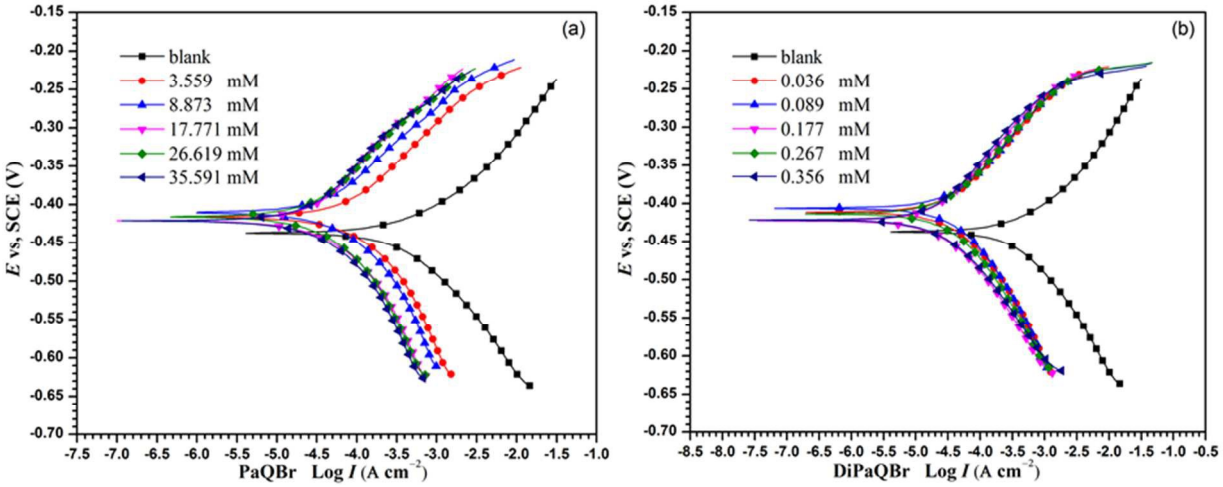

Fig. 5 Potentiodynamic polarization curves for N80 steel in 15 wt.% HCl without and with different concentrations of (a) PaQBr, (b) DiPaQBr at 25 °C.

Result in Table 2 shows that the corrosion current density (I_{corr}) decreases sharply with the increase in the concentration of both the two studied inhibitors, leading to the increase in the

View Article Online
DOI: 10.1039/C8NJ02505C

inhibition efficiency. The electrochemical reaction rate was reduced due to the formation of a barrier layer over the steel surface by the inhibitor molecule and both the two compounds act as good corrosion inhibitor in 15 wt.% HCl solution. Obviously, the inhibitive capability of DiPaQBr is much better than that of PaQBr, because the I_{corr} reaches a much lower value at a much lower concentration of DiPaQBr. Considering the active adsorption sites (nitrogen atoms, π-electrons, as well as the carbonyl groups) are reinforced in DiPaQBr, it is not surprising that this dimer derivative could display such a fine anticorrosive performance.

Table 2 Potentiodynamic parameters and inhibition efficiency for N80 steel in 15 wt.% HCl at 25 °C in the absence and presence of inhibitor

substance	Conc. (mM)	b_a (mV dec^{-1})	$-b_c$ (mV dec^{-1})	I_{corr} (μA cm^{-2})	$-E_{corr}$ (mV vs. SCE)	η (%)
15% HCl	0	85.9	126.8	985.9	437	
PaQBr	3.559	136.0	151.3	72.0	416	92.7
	8.873	132.2	133.7	43.4	411	95.6
	17.771	147.7	145.5	31.5	413	96.8
	26.619	155.2	152.5	27.6	417	97.2
	35.591	160.6	152.3	22.7	419	97.7
DiPaQBr	0.036	110.3	120.6	36.5	410	96.3
	0.089	111.4	132.0	30.8	406	96.9
	0.177	111.5	109.8	28.7	419	97.1
	0.267	116.5	124.5	29.1	413	97.0
	0.356	117.9	109.8	28.5	414	97.1

Inspection of Fig. 5 reveals that the polarization curves exhibit some shifts in potential towards more anodic regions relative to the blank solution. After a careful examination of the results in Table 2, it is easy to recognize that compared with the uninhibited group, the inhibited specimens did not show any significant change in values of E_{corr} as the largest shift in E_{corr} values were 27 mV and 31 mV for PaQBr and DiPaQBr respectively. According to literatures of corrosion,[50-51]

View Article Online
DOI: 10.1039/C8NJ02505C

the displacement of E_{corr} in Table 2 between blank and in presence of PaQBr or DiPaQBr lies within ±85 mV/SCE, indicating that the two inhibitors belong to mixed-type inhibitor.

From Table 2, it is clear that as the concentration of the two inhibitors changed, the values of anodic and cathodic Tafel slope constants (b_a and b_c) increase or decrease slightly. This implies that the mechanism of the corrosion reaction on both two electrodes was not changed clearly in the presence of PaQBr and DiPaQBr.[52] The irregular variation of the cathodic and anodic slopes in Table 2 reveal that the inhibition of steel was due to the adsorption of inhibitive molecules along with the blocking of active sites and the formation of complexes on the steel surface.[53] However, for both PaQBr and DiPaQBr, it is clear that the values of b_a are greatly affected compared with the value of b_c, which indicate that the two compounds can be considered as predominantly anodic type inhibitors.

3.5 EIS measurement

The Nyquist and Bode plots for the N80 steel corrosion in the absence and presence of PaQBr (or DiPaQBr) is shown in Fig. 6(a and b) and Fig. 7(a, b, c and d) respectively. It is evident that the inhibited and uninhibited specimens exhibit a single semicircular capacitive loop, indicating that the corrosion process of N80 steel in 15 wt.% HCl is under charge transfer control.[54] The appearance of Nyquist plots for N80 steel is very similar in uninhibited and the inhibited solution. This indicates that the inhibitors are retarding the corrosion process without changing the corrosive mechanism.

It is well known that in Nyquist plots the diameter of the capacitive loop represents the charge transfer resistance of the electrodes. The larger diameter of the impedance semicircle usually indicates a better corrosion prevention behavior.[55] Fig. 6 shows that the diameters of the capacitive loops in the inhibited solutions are bigger than that in the uninhibited group for both

View Article Online
DOI: 10.1039/C8NJ02505C

of the two inhibitors. This implies that the two studied compounds could exhibit an relatively good corrosion inhibition in 15 wt.% HCl solution. Besides, the shape and size of impedance semicircle in Fig. 6 is gradually increased with the addition of inhibitor, showing that the charge transfer resistance was increasing as the concentration of inhibitor rises. This phenomenon is also known as the reduction in the dissolution of the electrode, owning to the protective layer of inhibitors formed on the steel surface.[56]

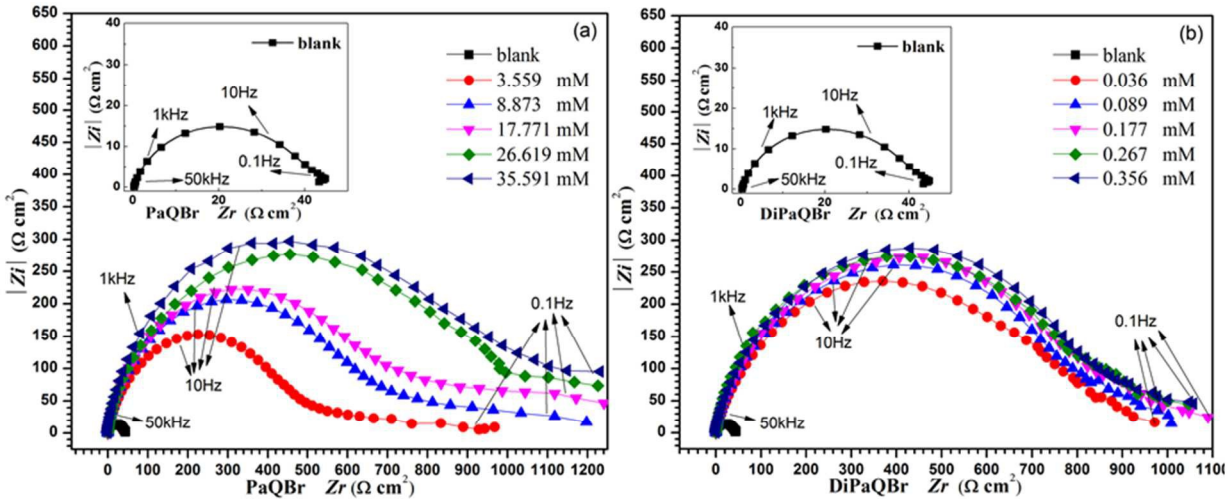

Fig. 6 Nyquist plot for N80 steel in 15 wt.% HCl without and with various concentrations of (a) PaQBr, (b) DiPaQBr as inhibitor at 25 °C.

For PaQBr, it is obvious in Fig. 6(a) that the diameter of the capacitive loop is proportional to the increasing concentration of the inhibitor. However, since DiPaQBr is slightly soluble in 15 wt.% HCl, the diameter of the impedance loop in Fig. 6(b) did not enlarge apparently in accordance with the increasing concentration of DiPaQBr. Nevertheless, it is not surprise to find in Fig. 6 that the diameter of the impedance semicircles of DiPaQBr is larger than that of PaQBr even when the concentration of DiPaQBr (0.036 mM) is only one percent of that of PaQBr (3.559 mM), which indicates that the inhibitive capability of DiPaQBr is much better than PaQBr.

View Article Online
DOI: 10.1039/C8NJ02505C

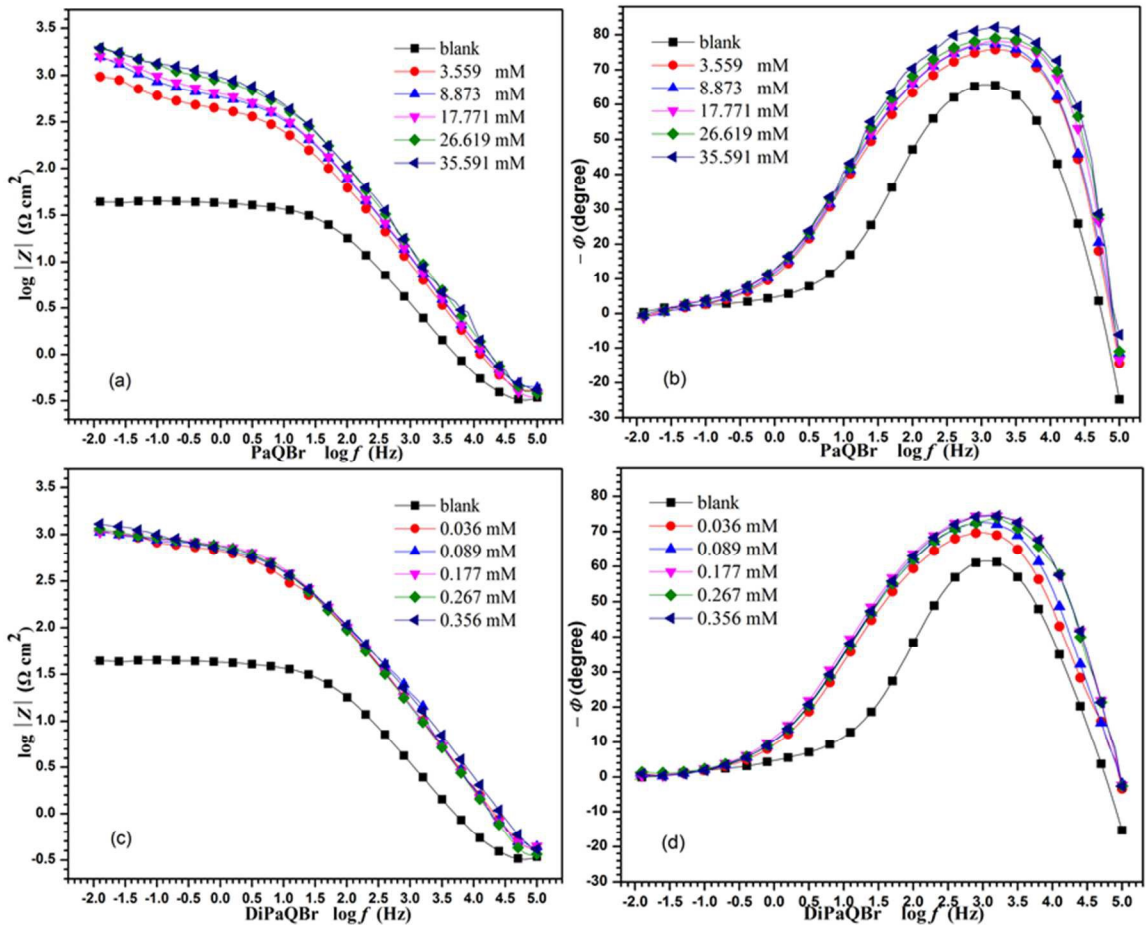

Fig. 7 The Bode plots for N80 steel in 15 wt.% HCl in the absence and presence of different concentrations of inhibitors at 25 °C: (a and b) PaQBr, (c and d) DiPaQBr.

The Bode impedance and phase angle plots for N80 steel in 15 wt.% HCl with and without inhibitors are given in Fig. 7. It is noticed that compared with the uninhibited blank group, both the impedance modulus Z_{mod} in Fig. 7(a, c) and Phase angle in Fig. 7(b, d) increased significantly when inhibitor was added. Both the PaQBr and DiPaQBr present the ability to prevent the specimen from severely corroded. For the two inhibitors, it can be seen in Fig. 7(b) and Fig. 7(d) that compared with the uninhibited specimen, the values of phase angles moved to more negative direction as the concentration of the inhibitors increased. This suggests that more

View Article Online
DOI: 10.1039/C8NJ02505C

inhibitive molecules were adsorbed onto the steel surface and the smoothness of the metal-solution interface was modified at higher concentration of inhibitors.[54-55]

Fig. 8 depicts the equivalent circuit model employed to simulate the experimental EIS results. The circuit consists of the solution resistance (R_s), the polarization resistance (R_p) and a constant phase element (CPE). The depressed semicircular Nyquist plot in the presence of inhibitors is considered as the polarization resistance between the steel surface and outer Helmholtz plane.[57] In that case, the polarization resistance (R_p) containing charge transfer resistance (R_{ct}), diffuse layer resistance (R_d), accumulation resistance (R_a) and film resistance (R_f) etc.[58] were included. CPE was used at the place of double layer capacitance (C_{dl}) to consider the roughness and other homogeneities of the electrode, dislocation, adsorption of inhibitors etc.

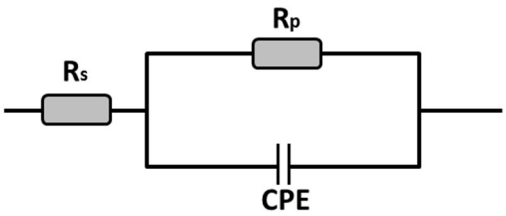

Fig. 8 Equivalent circuit model used to fit the EIS Nyquist plots.

The inhibition efficiencies (η) can be calculated by means of the following equation:[52]

$$\eta = \frac{R'_p - R_p}{R'_p} \times 100 \qquad (4)$$

where, R_p and R'_p are the polarization resistance of the steel in the absence and presence of the inhibitors, respectively. The representative example of using the equivalent circuit to fit the experimental data for N80 steel in 15wt. % HCl with 3.559 mM PaQBr and 0.036 mM DiPaQBr is shown in Fig. 9. The calculated EIS parameters are displayed in Table 3 according to the model circuit. It is clear that the very small value of the associated chi-square (χ^2) in Table 3 indicates the validity of the used circuit. As shown in Table 3, with the increasing concentration

View Article Online
DOI: 10.1039/C8NJ02505C

of the two inhibitors, the values of charge transfer resistance (R_p) increases while the electric double layer capacitance (C_{dl}) values decreases. The R_p values are observed to be proportional to the concentration of the two inhibitors and the gradual increase of R_p implies a greater blocking effect of the active area at the surface.[51-52] The inhibitor molecules could form a protective film on the metal surface by the adsorption and therefore, the transfer of charges from the metal surface to the corrosive medium becomes more difficult. The value of C_{dl} is related to the charge storage ability of the interface double layer. The decreasing tendency of C_{dl} values implies the reduction of charges accumulated in the double layer due to the adsorption of the inhibitor molecules.[52] Also, the decrease in C_{dl} reveals the decrease of the local dielectric constant or an increase in the thickness of the electrical double layer.[56] In addition, it is worth noticing that the inhibition efficiencies obtained from EIS measurement and the polarization methods are in good agreement among the two inhibitors.

Table 3. EIS parameters of N80 steel in 15wt. % HCl with and without various concentrations of PaQBr and DiPaQBr at 25 °C

substance	Conc. (mM)	R_s (Ω cm^2)	R_p (Ω cm^2)	C_{dl} (μF cm^{-2})	n	$\chi^2 \times 10^{-3}$	η (%)
15% HCl	0	1.13	21.2	129.5	0.75	1.13	
PaQBr	3.559	0.98	336.4	107.2	0.82	1.89	93.7
	8.873	1.06	509.3	89.8	0.69	2.01	95.8
	17.771	1.09	602.1	78.2	0.67	1.36	96.5
	26.619	0.89	727.9	68.1	0.59	1.58	97.1
	35.591	1.23	811.0	62.0	0.81	1.47	97.4
DiPaQBr	0.036	0.99	633.2	92.3	0.67	1.32	96.6
	0.089	0.95	660.0	88.1	0.85	1.68	96.8
	0.177	1.07	674.6	77.5	0.72	2.21	96.8
	0.267	1.11	696.2	64.5	0.91	0.99	96.9
	0.356	1.09	704.6	55.8	0.79	1.77	97.0

View Article Online
DOI: 10.1039/C8NJ02505C

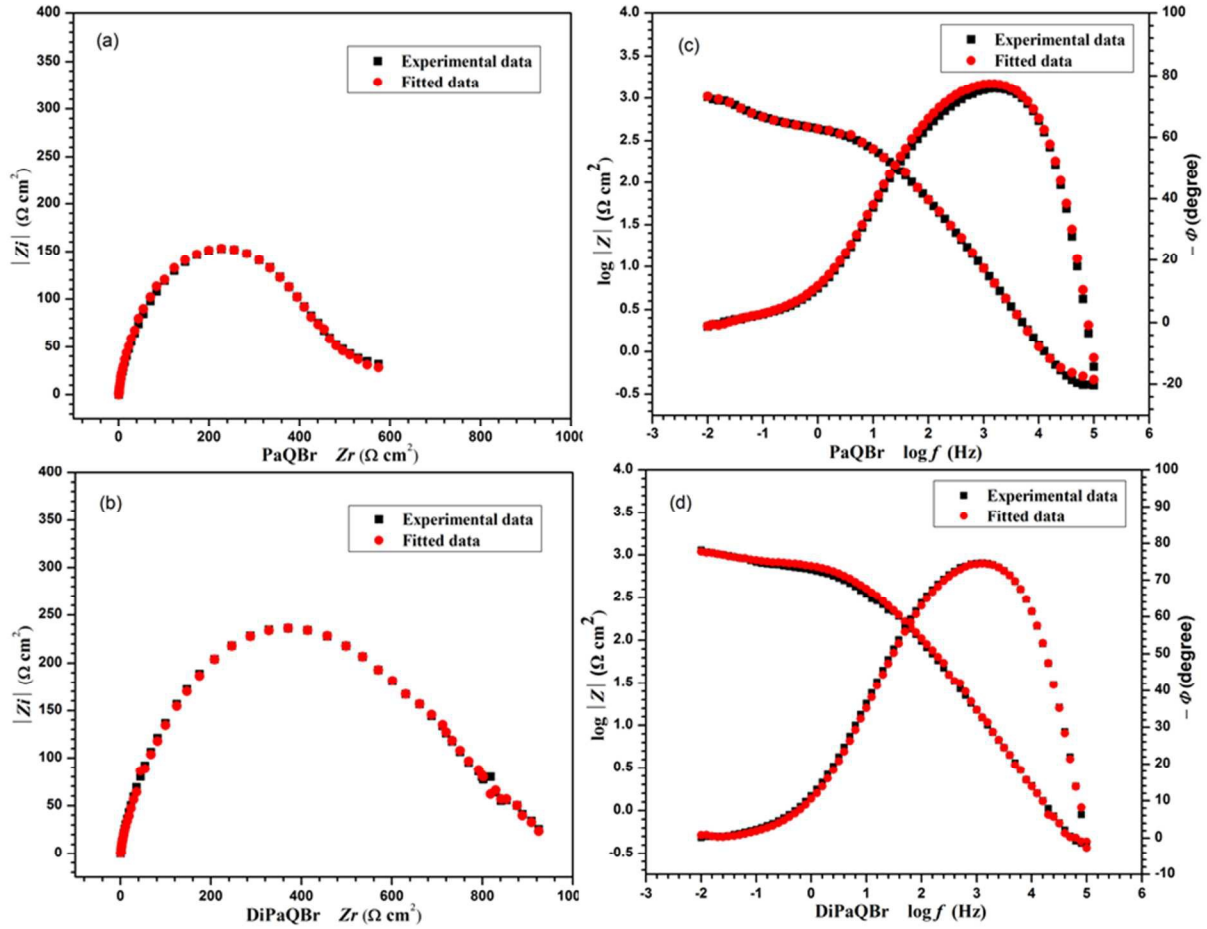

Fig. 9 The representative of example simulation of Nyquist and Bode plots for PaQBr at 3.559 mM (a and c) and DiPaQBr at 0.036 mM (b and d).

It can be summarized from the results of EIS measurements that after being transformed into the indolizine derivative, the anticorrosion performance of the heterocyclic quaternary ammonium inhibitor (PaQBr) gets promoted. Similar result also could be concluded in literature[1] where the inhibition of BQC and its indolizine derivative BQD was studied. The experimental results from previous work and this work indicates that the anti-corrosion ability of the indolizine derivative is far better than the original quaternary ammonium inhibitor (heterocyclic quaternary ammonium salts with active -CH_2- structure).

View Article Online
DOI: 10.1039/C8NJ02505C

3.6 Adsorption isotherms

In order to obtain the thermodynamic parameters about the adsorption process of the inhibitors, the relationship between the surface coverage (θ) and the concentration of the inhibitor (C) must be considered. In this work, several attempts (including Langmuir, Temkin, Frumkin and Freundlich isotherms) were made to find the relationship between θ and C according to the weight loss results in Table 1. The Langmuir adsorption isotherm was found to be the best one that fitted with the results based on the correlation coefficient (R^2).

According to the Langmuir adsorption isotherm, the relationship between θ and C can be expressed as following:[59]

$$\frac{C}{\theta} = \frac{1}{K_{\text{ads}}} + C \qquad (5)$$

From the equation, K_{ads} is the adsorption-desorption equilibrium constant for the adsorption process and C is the inhibitor concentration, θ represents the coverage area of the surface obtained from weight loss tests. From the intercept of the isotherm plot, the equilibrium constant (K_{ads}) could be acquired and therefore, the Gibbs standard free energy of adsorption (ΔG^0_{ads}) can be determined by K_{ads} using the following equation:

$$\ln K_{\text{ads}} = \ln \frac{1}{55.5} - \frac{\Delta G^0_{\text{ads}}}{\text{RT}} \qquad (6)$$

where, R is the general gas constant, T is the absolute temperature and 55.5 is the molar concentration of water in solution in mol L^{-1}.[60] The plots of C/θ against C for the two inhibitors are shown in Fig. 10 and the thermodynamic parameters are given in Table 4.

View Article Online
DOI: 10.1039/C8NJ02505C

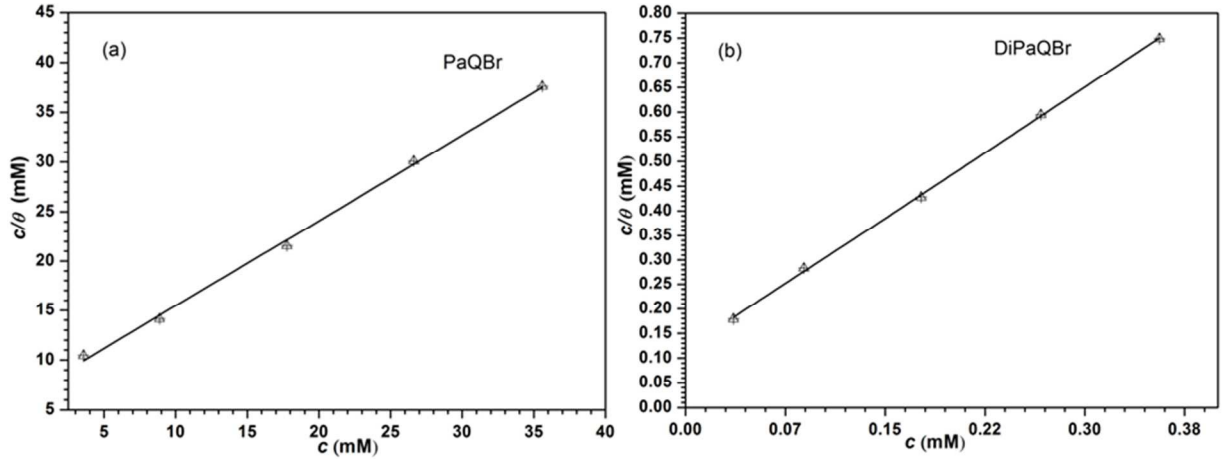

Fig. 10 Langmuir adsorption isotherm plot of N80 steel obtained in 15 wt.% HCl with the addition of different concentrations of (a) PaQBr and (b) DiPaQBr as inhibitor at 90 °C.

For PaQBr and DiPaQBr, the obtained plots is found to be perfectly linear with the correlation coefficient (R^2) higher than 0.999. This indicates that both the two inhibitors obey the Langmuir adsorption isotherm. As shown in Table 4, the standard free energy (ΔG^0_{ads}) are -27.17 kJ mol^{-1} for PaQBr and -39.42 kJ mol^{-1} for DiPaQBr, the negative sign for ΔG^0_{ads} refers to the spontaneous adsorption of the inhibitors.

Table 4. Adsorption parameters of the adsorption process of PaQBr and DiPaQBr

substance	R^2	$K_{ads}/(L\ mol^{-1})$	$\Delta G^0_{ads}/(kJ\ mol^{-1})$
PaQBr	0.9993	145.81	- 27.17
DiPaQBr	0.9995	8422.47	- 39.42

In general, when the magnitude of ΔG^0_{ads} for the inhibitor lies in the order of -20 kJ mol^{-1} or more positive, it satisfies the physisorption between the inhibitor and the metal surface. The ΔG^0_{ads} values around -40 kJ mol^{-1} or more negative are associated with the chemisorption process.[55] Considering the above description and the calculated ΔG^0_{ads} values in Table 4, it can be claimed that DiPaQBr (ΔG^0_{ads} = -39.42 kJ mol^{-1}) closely exhibits the chemical adsorption with

View Article Online
DOI: 10.1039/C8NJ02505C

the steel surface in 15 wt. % HCl, while the type of interaction between PaQBr (ΔG^0_{ads} = -27.17 kJ mol^{-1}) and the metallic surface included physisorption as well as chemisorption.[59]

3.7 Suggested mechanism of inhibition

Electron-rich atoms such as nitrogen, sulfur, oxygen, etc.[2,4,60-62] and conjugated structures containing π-electrons are main functional groups of inhibitors for metal or alloy. Quaternary N^+ cation, the oxygen atom in carbonyl group as well as the aromatic π-electrons are key inhibitive groups[63-65] in PaQBr and its indolizine derivative. The unshared electron pair and π-conjugated electrons would coordinate with the empty d-orbital in metal atoms, which the adsorption is classified as chemical adsorption. The firmly adsorbed inhibitors would thereby prohibit the metal surface from the contact of H^+ ions. By comparison of PaQBr and BQC,[1,10] the extra adsorbing sites and the beneficial synergistic effect of Br^- lead to a great rise in corrosion prevention. These are the main reasons why PaQBr shows a better inhibitive performance than that of BQC.

The observed corrosion inhibition of N80 steel in 15 wt. % HCl in the presence of PaQBr or DiPaQBr can be explained by the adsorption of the inhibitor and the mechanism of the inhibition process is discussed by Bockris, Drazic and Despic (BDD) mechanism.[66]

As is proposed in the potentiodynamic polarization result, the hydrogen evolution process is activation-controlled and the mechanism of reduction is not affected even in the presence of the two inhibitors. Probable protocols of the cathodic electrode reaction can be abridged as follows:

$$Fe + H^+ + e^- \leftrightarrow (FeH)_{ads} \quad (7)$$

$$Fe + (In^+)_{ads} + e^- \rightarrow (Fe \cdot In)_{ads} \quad (8)$$

$$(FeH)_{ads} + H^+ + e^- \rightarrow Fe + H_2 \quad (9)$$

View Article Online
DOI: 10.1039/C8NJ02505C

where, the subscript 'ads' represents the adsorption on the surface of steel, 'In^+' represents the inhibitive cation. It is apparent from the Eq. (7) and Eq. (8) that there is a competition between H^+ and In^+ to get adsorbed onto the metal surface. Since the first step (Eq. 7) is very likely to be the rate-controlling step, the presence of the inhibitor in the acidic solution retards the hydrogen reduction. The high molecular weight and large size of the studied inhibitor also increases the inhibition efficiency.

The mechanism for the anodic dissolution of Fe in acidic solution was proposed initially in literature.[66-67] In the presence of inhibitor, the mechanism for the retardation of Fe anodic dissolution can be proposed as follows:

$$Fe + H_2O \leftrightarrow (Fe \cdot H_2O)_{ads} \quad (10)$$

$$(Fe \cdot H_2O)_{ads} + In \leftrightarrow (FeOH^-)_{ads} + H^+ + In \quad (11)$$

$$(Fe \cdot H_2O)_{ads} + In \leftrightarrow (FeIn)_{ads} + H_2O \quad (12)$$

$$(FeOH^-)_{ads} \xrightarrow{rds} (FeOH)_{ads} + e^- \quad (13)$$

$$(FeIn)_{ads} \leftrightarrow (FeIn^+)_{ads} + e^- \quad (14)$$

$$(FeOH)_{ads} + (FeIn^+)_{ads} \leftrightarrow (FeIn)_{ads} + FeOH^+ \quad (15)$$

$$FeOH^+ + H^+ \leftrightarrow Fe^{2+} + H_2O \quad (16)$$

where, 'In' represents the inhibitor molecule. According to the above mechanism, the formation of the adsorbed intermediate $FeIn_{ads}$ (Eq. 12) reduces the amount of $FeOH^-{}_{ads}$ (Eq. 11) available for the key rate determining step (Eq. 13). Depending on the relative solubility of the adsorbed intermediate, $FeIn_{ads}$ could either inhibit or catalyze the further dissolution of the metal. From the experimental results, it can be inferred that the insoluble complexes of Fe-PaQBr or Fe-DiPaQBr dominates the intermediates and thus enhances the inhibitive effects.

View Article Online
DOI: 10.1039/C8NJ02505C

As a condensed dimer derivative of PaQBr, the active adsorption sites (nitrogen atoms, π-electrons, as well as the carbonyl groups) in PaQBr are reinforced in DiPaQBr. As a result, the indolizine derivative DiPaQBr could provide more adsorption sites than that of PaQBr. The extra adsorption sites in the dimer derivative would fasten the inhibitor with the crude surface and finally increases the inhibitive ability. Although a stronger protective interaction would occur between the DiPaQBr and the steel, the relatively low solubility of DiPaQBr (containing two hydrophobic carbonyl groups) make it less effective to present its inhibitive potentiality.

3.8 Comparison of inhibitory efficiencies of some heterocyclic quaternary ammonium salts inhibitors in acidic solution

Table 5 shows the inhibitory efficiencies of the studied inhibitor and some of the reported similar heterocyclic quaternary ammonium inhibitor for N80 steel in 15 wt.% HCl. It is clear from the table that the prepared compound could exhibit a relatively better corrosion protection than those of the analogous inhibitive N-heterocyclic quaternary ammonium salts in literature.

Table 5. Some heterocyclic quaternary ammonium salts investigated as corrosion inhibitors in literatures and this work for N80 steel in 15 wt.% HCl (by weight loss mesaurment)

Name of the inhibitor	Inhibition efficiency (%)	Reference
1-benzylquinlinium chloride	80.6	1, 10
N-dodecylpyridinium bromide	91.5	2
N,N′-Butane-1,4-diyl-bisquinolinium dibromide	81.1	4
N,N′-Butane-1,6-diyl-bisquinolinium dibromide	86.1	4
N,N′-Butane-1,8-diyl-bisquinolinium dibromide	91.0	4
1-naphthylmethylquinolinium chloride	92.5	68
(4-vinyl)-benzyl quinoidine chloride	76.9	69
Phenacyl Quinolinium Bromide	94.7	This work

View Article Online
DOI: 10.1039/C8NJ02505C

4. Conclusion

DiPaQBr, the dimer indolizine derivative of a strong acid corrosion inhibitor Phenacyl Quinolinium Bromide (PaQBr) was synthesized from PaQBr. Through HRMS and NMR, the structure of DiPaQBr was characterized and determined as $C_{34}H_{23}N_2O_2Br$. The corrosion inhibition of PaQBr and DiPaQBr in 15 wt.% HCl were evaluated by weight loss measurement, potentiodynamic polarization and EIS measurement. Based on the experimental results, the following conclusions can be made:

(1) With the assistance of triethylamine, heterocyclic quaternary ammonium salts (PaQBr) with active methylene group could get converted to its dimer derivatives (DiPaQBr). The dimer derivative could be classified as indolizine quaternary ammonium salt. The formation mechanism of DiPaQBr from the condensation of two molecules of PaQBr through 1,3-dipolar cycloaddition was proposed and confirmed.

(2) It is evident that the corrosion inhibition of DiPaQBr is better than the PaQBr, since the DiPaQBr could reduce the corrosion rate to a lower value at a much lower concentration in gravimetric analysis. EIS results also showed that the DiPaQBr exhibits a greater inhibitive capability than PaQBr. Either PaQBr or DiPaQBr acted as a mixed-type inhibitor and retards the corrosion process without changing the corrosive mechanism. The results obtained from weight loss measurement and electrochemical methods are in agreement and confirm the big inhibition difference between PaQBr and its indolizine derivative DiPaQBr.

(3) It can be inferred that through 1,3-dipolar cycloaddition, the other heterocyclic quaternary ammonium salt inhibitors (including pyridine, quinoline and iso-quinoline salts etc.) which contain active methylene group may get converted to the corresponding inhibitive indolizine

View Article Online
DOI: 10.1039/C8NJ02505C

derivatives. In that way, using the dimer indolizine derivative as the novel corrosion inhibitors may offer a new method for corrosion protection in acid medium.

Conflicts of interests

The authors declare no competing financial interest.

Acknowledgement

Supported by “the Fundamental Research Funds for the Central Universities” (16CX06030A). Special thanks for Ren Sumei and Song Ni from Ocean University of China (OUC) for their smart work on HRMS and NMR experiments. Thanks for Yang Menglong, Yang Haiyan from Qingdao Institute of Bioenergy and Bioprocess Technology (QIBEBT) of the Chinese Academy of Sciences (CAS) for their assistance and helpful discussion on preparative chromatography. The author also express thanks to Sun Shuangqing, Tang Shiming and Xi Yanyan from China University of Petroleum (UPC) for their technical guidance on electrical and instrumental tests.

References

1 Z. Yang, F. T. Zhan, Y. Pan, Z. F. LYu, C.Y. Han, Y. P. Hu, P. P. Ding, T G. Gao, X. Y. Zhou and Y. N. Jiang, Structure of a novel Benzyl Quinolinium Chloride derivative and its effective corrosion inhibition in 15 wt.% hydrochloric acid, Corros. Sci., 2015, 99, 281-294.

2 M. Finšgar and J. Jackson, Application of corrosion inhibitors for steels in acidic media for the oil and gas industry: a review, Corros. Sci., 2014, 86, 17-41.

View Article Online
DOI: 10.1039/C8NJ02505C

3 P. Mourya, P. Singh, A. K. Tewari, R. B. Rastogi and M. M. Singh, Relationship between structure and inhibition behavior of quinolinium salts for mild steel corrosion: Experimental and theoretical approach, Corros. Sci., 2015, 95, 71-87.

4 X. Y. Zhang, Y. X. Zheng, X. P. Wang, Y. F. Yan and W. Wu, Corrosion inhibition of N80 steel using novel diquaternary ammonium salts in 15% hydrochloric acid, Ind. Eng. Chem. Res., 2014, 53, 14199-14207.

5 S. M. Elhadi, M. Bilel, B. Abdelmalek and C. Aissa, Experimental evaluation of quinolinium and isoquinolinium derivatives as corrosion inhibitors of mild steel in 0.5 M H_2SO_4 solution, Prot. Met. Phys. Chem. Surf., 2016, 52, 731-736.

6 G. Q. Xia, X. H. Jiang, L. M. Zhou, Y. W. Liao, M. Duan, H. Wang, Q. Pu and J. Zhou, Synergic effect of methyl acrylate and N-cetylpyridinium bromide in N-cetyl-3-(2-methoxycarbonylvinyl)pyridinium bromide molecule for X70 steel protection, Corros. Sci., 2015, 94, 224-236.

7 L. P. Crawford, E. B. Barmatov, T. L. Hughes and M. Y. Ho, Corrosion inhibition, in: UK Patent GB 2537597 A, October 26, 2016.

8 S. D. Wadekar and N. K. Pandya, Synergistic corrosion inhibitor intensifiers for acidizing emulsions, in US Patent 0116 708 A1, May 1, 2014.

9 O. V. Ugryumov, O. A. Varnavskaya, V. N. Khlebnikov, Y. N. Kamzina, D. N. Lebedev, G. V. Romanov, Y. V. Ivshin, R. A. Kaidrikov, F. S. Shakirov and F. I. Dautov, Corrosion Inhibitors of the SNPKh Type. 1. Development and Study of the Protective Effects of Corrosion Inhibitors Based on Heterocyclic Nitrogen-Containing Compounds, Prot. Met., 2005, 41, 69-73.

View Article Online
DOI: 10.1039/C8NJ02505C

10 F. T. Zhan, Z. Yang, Z. F. Lü, Y. P. Hu, Y. Pan, Y. F. Chen, C. L. Xiao and T. Zhang, Preparation and characterization of N-Benzylquinolinium Chloride Derivative (BQD) with effective corrosion inhibition, Acta. Petrol. Sin., 2015, 36, 1116-1121. (in Chinese).

11 T. Uchida and K. Matsumoto, Methods for the construction of the indolizine nucleus, Synthesis, 1976, 4, 209-236.

12 M. Shipman, Product class 16: indolizines, Sci. Synth., 2001, 10, 745-787.

13 J. Fröhlich and F. Kröhnke, Indolizine aus phenacyl-cyclimoniumsalzen, Chem. Ber., 1971, 104, 1621-1628.

14 H. Quast and A. Gelléri, Heterocyclische Ylide, IV. Decarboxylierung von 1-methylchinolinium-2-carboxylat in Abwesenheit Elektrophiler Reagenzien, Justus Liebigs Annalen Der Chemie, Eur. J. Org. Chem., 1975, 5, 929-938.

15 H. Quast and A. Gelléri, Heterocyclische Ylide, V. Cycloaddition von N-Chinoliniummethylid an N-methylchinoliniumkationen, Justus Liebigs Annalen der Chemie, Eur. J. Org. Chem., 1975, 5, 939–945.

16 K. Afarinkia, M.-R. Ansari, C. W. Bird and I. Gyambibi, A reinvestigation of the structure of the erythro and xanthoapocyanine dyes: some unusual aspects of quinoline chemistry, Tetrahedron Lett., 1996, 37, 4801-4804.

17 F. Kröhnke, H. Dickhäuser and I. Vogt, Zur Konstitution der sogenannten Xantho-apocyanine, Justus Liebigs Annalen der Chemie, Eur. J. Org. Chem., 1961, 644, 93-108.

18 F. Kröhnke, Syntheses using pyridinium salts, Angew. Chem. Int. Ed., 1963, 2, 225-238.

View Article Online
DOI: 10.1039/C8NJ02505C

19 D. S. Allgäuer, P. Mayer and H. Mayr, Nucleophilicity parameters of pyridinium ylides and their use in mechanistic analyses, J. Am. Chem. Soc., 2013, 135, 15216-15224.

20 R. I. Yurchenko, I. S. Pogrebova, T. N. Pilipenko and E. M. Kras'ko. Corrosion-protective properties of N-Phenacylmethylpyridinium Bromides, Russ. J. Appl. Chem., 2003, 76, 1764-1768.

21 R. I. Yurchenko, A. V. Dolina and A. G. Yurchenko. Inhibiting action of 1-Phenacylmethyl-2-R-Quinolinium Bromides at steel acid corrosion, Russ. J. Appl. Chem., 2011, 84, 2011-2012.

22 R. I. Yurchenko, A. V. Dolina and A. G. Yurchenko. Intermolecular synergy effect on the inhibiting action of N-Phenacylmethylquinolinium halides, Russ. J. Appl. Chem., 2011, 84, 2013-2014.

23 F. Kröhnke and W. Zecher, Syntheses using the michael adddition of pyridinium salts, Angew. Chem. Int. Ed., 1962, 1, 626-632.

24 J. W. Bunting and W. G. Meathrel, Quaternary nitrogen heterocycles. V. Substituent effects on the equilibrium constants for pseudobase formation from quinolinium and isoquinolinium cations, Can. J. Chem., 1974, 52, 962-974.

25 F. Shahrekipour, R. Heydari, B.Tahamipour, H. Saravani and C. Graiff, Efficient synthesis of new stable 1,4-diionic organosulfurs and corresponding mesoionic compounds from N-heterocyclic ylides, Phosphorus, Sulfur Silicon Relat. Elem., 2014, 189, 263-273.

26 J. Jacobs, E. V. Hende, S. Claessens and N. D. Kimpe, Pyridinium ylids in heterocyclic synthesis, Curr. Org. Chem., 2011, 15, 1340-1362.

View Article Online
DOI: 10.1039/C8NJ02505C

27 E. Georgescu, C. Draghici, P. C. Iuhas and F. Georgescu, A new approach for the synthesis of benzo[f]pyrrolo[1,2-a]-quinolines, ARKIVOC, 2005, X, 95-104.

28 W. Augstein and F. Kröhnke, Synthesen des Benzo[a]- und des Naphtho[2.3-b]indolizin-Ringsystems, Justus Liebigs Annalen der Chemie, Eur. J. Org. Chem., 1966, 697, 158-170.

29 Dieter-Bernd Reuschling and F. Kröhnke, Ringschlüsse unter HNO_2-abspaltung und C–C-Verknüpfung, II. Synthese neuer ringsysteme, Chem. Ber., 1971, 104, 2103–2109.

30 X. Huang and T. X. Zhang, Multicomponent reactions of pyridines, a-bromo carbonyl compounds and silylaryl triflates as aryne precursors: a facile one-pot synthesis of pyrido[2,1-a]isoindoles, Tetrahedron Lett., 2009, 50, 208-211.

31 S. Liu, X. G. Hu, X. H. Li and J. Cheng, Facile synthesis of pyrido[2,1-a]isoindoles via iron-mediated 2-Arylpyridine C–H bond cleavage, Synlett, 2013, 47, 0847-0850.

32 A. Maity, D. Chakraborty, A. Hazra, Y. P. Bharitkar, S. Kundu, P. R. Maulik and N. B. Mondal, Novel betaines/mesoionic compounds via a simple and convenient MCR in aqueous micellar system: synthesis of thiazolo[2,3-a] isoquinolin-4-ium derivatives, Tetrahedron Lett., 2014, 55, 3059-3063.

33 R. Z. Liu, X. Y. Wang, J. Sun and C. G. Yan, A facile synthesis of tricyclic skeleton of alkaloid 261C by double[3+2] cycloaddition of pyridinium ylide，Tetrahedron Lett., 2015, 56, 6711-6714.

34 A. S. Al-Bogami and A. S. El-Ahl, Microwave-mediated regiospecific synthesis of some novel annulated Spiro[indoline-3,1'-indolizin]-2-ones, Lett. Org. Chem., 2015 12, 2-12.

View Article Online
DOI: 10.1039/C8NJ02505C

35 L. Wu, J. Sun and C. G. Yan, Facile synthesis of spiro[indoline-3,3′-pyrrolo[1,2-a]quinolines] and spiro[indoline-3,1′-pyrrolo[2,1-a]isoquinolines] via 1,3-dipolar cycloaddition reactions of heteroaromatic ammonium salts with 3-phenacylideneoxindoles, Org. Biomol. Chem., 2012, 10, 9452-9463.

36 B. X Wang, T. He and H. W. Hu, Synthesis of naphtho[2,3-a]indolizine-7,12-quinones by the reaction of pyridinium N-Ylides with 1,4-Naphthoquinone in the presence of tetrakispyridine cobalt (II) dichromate, Acta Chim. Sinica., 2003, 61, 889-892. (in Chinese).

37 J. V. Grigoryan, G. T. Sargsyan, A. Kh. Gyulnazaryan, R. V. Paronikyan and G. M. Stepanyan, Synthesis and Antibacterial properties of several unsaturated quaternary ammonium salts. Pharm. Chem. J., 2013, 47, 25-28.

38 C. S. Kim and S. Y Hong, Kinetics and mechanism for reactions of substituted phenacyl bromides with quinoline, J. Korean Chem. Soc., 1984, 28, 265-268.

39 J. L. Hartwell and S. R. L. Kornberg, Some quaternary ammonium salts of heterocyclic bases, J. Am. Chem. Soc., 1946, 68, 868-870.

40 E. Pretsch, P. Bühlmann and M. Badertscher, Structure determination of organic cobmpounds: tables of spectral data, 4th edition (revised and enlarged edition), Sci. Press (Beijing) 2012; 274-275.

41 O. Tsuge, S. Kanemasa and S. Takenaka, Stereoselective synthesis of hexa- and tetrahydroindolizin-7-ones through cycloaddition of pyridinium methylides, J. Org. Chem., 1986, 51, 1853-1855.

View Article Online
DOI: 10.1039/C8NJ02505C

42 I. I. Druta, M. A. Andrei, C. I. Ganj and P. S. Aburel, Synthesis of indolizine derivatives by the reaction of 2-(2'-Pyridyi)-pyridinium ylides with ethylenic dipolarophiles, Tetrahedron, 1999, 55, 13063-13070.

43 J .F. Xu, H. Y. Hu, Y. Liu, X. Wang, Y. H. Kan and C. Wang, Four-component reaction for the synthesis of indolizines by copper-catalyzed aerobic oxidative dehydrogenative aromatization, Eur. J. Org. Chem., 2017, 2017, 257-261.

44 B. X Wang, J. X. Hu, Y. F. Hu and H. W. Hu, A Facile One-step synthesis of 1-Acylindolizines by the reaction of pyridinium salts with mannich bases in the presence of TPCD, Chem. J. Chinese U., 1999, 20, 418-420. (in Chinese).

45 P. Mourya, S. Banerjee and M. M. Singh, Corrosion inhibition of mild steel in acidic solution by Tagetes erecta (Marigold flower) extract as a green inhibitor, Corros. Sci., 2014, 85, 352-363.

46 M. T. Alhaffar, S. A. Umoren, I. B. Obotb and S. A. Ali, Isoxazolidine derivatives as corrosion inhibitors for low carbon steel in HCl solution: experimental, theoretical and effect of KI studies, RSC Adv., 2018, 8, 1764-1777.

47 A. Khamis, M. M. Saleh, and M. I. Awad, Synergistic inhibitor effect of cetylpyridinium chloride and other halides on the corrosion of mild steel in 0.5 M H_2SO_4, Corros. Sci., 2013, 66, 343-349.

48 X. H. Li, X. G, Xie, S. D. Deng and G. B. Du, Inhibition effect of two mercaptopyrimidine derivatives on cold rolled steel in HCl solution, Corros. Sci., 2015, 92, 136-147.

View Article Online
DOI: 10.1039/C8NJ02505C

49 A. Pandey, B. Singh, C. Vermabc and E. E. Ebenso, Synthesis, characterization and corrosion inhibition potential of two novel Schiff bases on mild steel in acidic medium, RSC Adv., 2017, 7, 47148-47163.

50 K. G. Zhang, B. Xu, W. Z. Yang, X. S. Yin, Y. Liu and Y. Z. Chen, Halogen-substituted imidazoline derivatives as corrosion inhibitors for mild steel in hydrochloric acid solution, Corros. Sci., 2015, 90, 284-295.

51 T. R. Wang, J. L. Wang and Y. Q. Wu, The inhibition effect and mechanism of l-cysteine on the corrosion of bronze covered with a CuCl patina, Corros. Sci., 2015, 97, 89-99.

52 M. M. Solomon, S. A. Umoren and E. J. Abai, Poly(methacrylic acid)/silver nanoparticles composites: In-situ preparation, characterization and anticorrosion property for mild steel in H_2SO_4 solution, J. Mol. Liq., 2015, 212, 340-351.

53 R. Kumar, H. Kim, and G. Singh, Experimental and theoretical investigations of a newly synthesized azomethine compound as inhibitor for mild steel corrosion in aggressive media: A comprehensive study, J. Mol. Liq., 2018, 259, 199-208.

54 J. Haque, V. Srivastava, C. Verma, H. Lgaz, R. Salghi, and M. A. Quraishi, N-Methyl-N,N,N-trioctylammonium chloride as a novel and green corrosion inhibitor for mild steel in an acid chloride medium: electrochemical, DFT and MD studies, New J. Chem., 2017, 41, 13647-13662.

55 A. Kumar, M. Trivedi, Bhaskaran, R. K. Sharma, and G. Singh, Synthetic, spectral and structural studies of a Schiff base and its anticorrosive activity on mild steel in H_2SO_4, New J. Chem., 2017, 41, 8459-8468.

View Article Online
DOI: 10.1039/C8NJ02505C

56 M. A. Hegazy, A. S. El-Tabei, A. H. Bedair and M. A. Sadeq, Synthesis and inhibitive performance of novel cationic and gemini surfactants on carbon steel corrosion in 0.5 M H_2SO_4 solution, RSC Adv., 2015, 5, 64633–64650.

57 M. Das, A. Biswas, B. K. Kundu, S. M. Mobin, G. Udayabhanu and S. Mukhopadhyay, Targeted synthesis of cadmium(II) Schiff base complexes towards corrosion inhibition on mild steel, RSC Adv., 2017, 7, 48569-48585.

58 M. A. Hegazy, A. Y. El-Etre, M. El-Shafaie and K. M. Berry, Novel cationic surfactants for corrosion inhibition of carbon steel pipelines in oil and gas wells applications, J. Mol. Liq., 2016, 214, 347-356.

59 B. Maleki, A. Davoodi, M. V. Azghandi, M. Baghayeri, E. Akbarzadeh, H. Veisi, S. S. Ashrafi and M. Raei, Facile synthesis and investigation of 1,8-dioxooctahydroxanthene derivatives as corrosion inhibitors for mild steel in hydrochloric acid solution, New J. Chem., 2016, 40, 1278-1286.

60 N. K. Gupta, C. Verma, R. Salghi, H. Lgaz, A. K. Mukherjee and M. A. Quraishi, New phosphonate based corrosion inhibitors for mild steel in hydrochloric acid useful for industrial pickling processes: experimental and theoretical approach, New J. Chem., 2017, 41, 13114-13129.

61 A. Khamis, M.M. Saleh, M.I. Awad and B.E. EI-Anadouli, Enhancing the inhibition action of cationic surfactant with sodium halides for mild steel in 0.5 M H_2SO_4, Corros. Sci., 2013, 74, 83-91.

View Article Online
DOI: 10.1039/C8NJ02505C

62 M. Prabakaran, S. H. Kim, A. Sasireka, V. Hemapriyac and I. M. Chung, beta-Sitosterol isolated from rice hulls as an efficient corrosion inhibitor for mild steel in acidic environments, New J. Chem., 2017, 41, 3900-3907.

63 Y. Pan, F. T. Zhan, Z. F. Lu, Y. Lin, Z. Yang and Z. Wang, A Mannich base 1-phenyl-3-(1-pyrrolidinyl)-1-propanone: synthesis and performance study on corrosion inhibition for N80 steel in 15% hydrochloric acid, Anti-Corros. Method M., 2016, 63, 153-159.

64 A. Kokalj, S. Peljhan, M. Finšgar and I. Milošev, What determines the inhibition effectiveness of ATA, BTAH, and BTAOH corrosion inhibitors on Copper?, J. Am. Chem. Soc., 2010, 132, 16657-16668.

65 S. Ramachandran, B.L. Tsai, M. Blanco, H. Chen and Y. C. Tang, W.A. Goddard, Self-assembled monolayer mechanism for corrosion inhibition of iron by imidazolines, Langmuir, 1996, 12, 6419-6428.

66 J. O'M. Bockris, D. Drazic and A. R. Despic, The electrode kinetics of the deposition and dissolution of iron, Electrochim. Acta, 1961, 4, 325-361.

67 P. C. Okafor, M. E. Ikpi, I. E. Uwah, E. E. Ebenso, U. J. Ekpe and S. A. Umoren, Inhibitory action of Phyllanthus amarus extracts on the corrosion of mild steel in acidic media, Corros. Sci., 2008, 50, 2310-2317.

68 C. Sitz, W. Frenier, C. Vallejo, Acid corrosion inhibitors with improved environmental profiles, in: SPE 155966. Society of Petroleum Engineers International Conference and Exhibition on Oilfield Corrosion, Aberdeen, UK, May 28-29, 2012.

View Article Online
DOI: 10.1039/C8NJ02505C

69 P. Jiang, L. Y. Zhao, Z. H. Wan, J. J. Ge, P. Zong, J. J. Liu and S. Z. Li, Researches on Inhibiting Action of Quinolinic Quatermary Ammonium Salts, Oilfield Chemistry, 2011, 28, 219-223. (in Chinese).

View Article Online
DOI: 10.1039/C8NJ02505C

For Table of Content ONLY

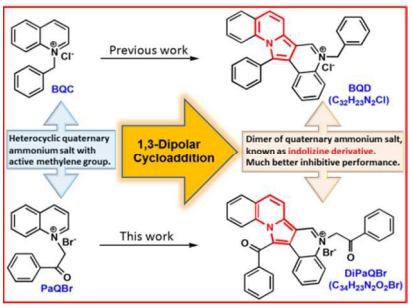

The anti-corrosion inhibition was dramatically improved as the heterocyclic ammonium inhibitors get transformed into their dimer indolizine derivative.